

## “Modular Cascaded H-Bridge Multilevel Photovoltaic Inverter with Distributed Maximum power point tracking for Single/Three Phase Grid-Connected Applications”

R. Blessina Preethi<sup>1</sup> T. Thenmozhi<sup>2</sup>,

<sup>1</sup>(Assistant Professor (Dept of ECE), SVP CET, AP).

<sup>2</sup>(Assistant Professor (Dept of ECE), SVP CET, AP)

**Abstract:** A grid-connected photovoltaic power system, or grid-connected photovoltaic system is an electricity generating system that is connected to the utility grid. A grid-connected PV system consists of solar panels, one or several inverters, a power conditioning unit and grid connection equipment. Hence to improve the efficiency and flexibility of PV systems this paper presents a modular cascaded H-bridge multilevel photovoltaic (PV) inverter for single- or three-phase grid-connected applications. The modular cascaded multilevel topology helps to improve. To realize better utilization of PV modules and maximize the solar energy extraction, a distributed maximum power point tracking control scheme is applied to both single- and three-phase multilevel inverters, which allows independent control of each dc-link voltage. For three-phase grid-connected applications, PV mismatches may introduce unbalanced supplied power, leading to unbalanced grid current. To solve this issue, a control scheme with modulation compensation is also proposed. An experimental three-phase seven-level cascaded H-bridge inverter has been built utilizing nine H-bridge modules (three modules per phase). Each H-bridge module is connected to a 185-W solar panel. Simulation and experimental results are presented to verify the feasibility of the proposed approach.

**Keywords:** Cascaded multilevel inverter, distributed maximum power point (MPP) tracking (MPPT), modular, modulation compensation, photovoltaic (PV).

---

### NOMENCLATURE

$I_{qref}$	reactive current reference
$I_{dref}$	current reference
PI	proportional–integral
PLL	phase locked loop
$di$	modulation index
$P_{in}$	phase input power
$P_{inav}$	average input power
$V_{rms}$	Root mean square voltage
THD	total harmonic distortion
$v_{jN}$	inverter output voltage
$n$	number of H-bridge modules per phase
$v_{jN}$	output voltage of the three-phase inverter
$r_j$	ratio of unbalanced power

### I. INTRODUCTION

Due to shortage of fossil fuels and environmental problems caused by conventional power generation, renewable energy, particularly solar energy has become very popular. Solar-electric-energy demand has grown consistently by 20%–25% per annum over the past 20 years [1], and the growth is mostly in grid-connected applications. With the extraordinary market growth in grid-connected photovoltaic (PV) systems, there are increasing interests in grid-connected PV configurations.

Five inverter families can be defined, which are related to different configurations of the PV system: 1) central inverters; 2) string inverters; 3) multistring inverters; 4) ac-module inverters; and 5) cascaded inverters [2]–[7]. The configurations of PV systems are shown in Fig. 1.

Cascaded inverters consist of several converters connected in series; thus, the high power and/or high voltage from the combination of the multiple modules would favor this topology in medium and large grid-connected PV systems [8]–[10]. There are two types of cascaded inverters. Fig. 1(e) shows a cascaded dc/dc converter connection of PV modules [11], [12]. Each PV module has its own dc/dc converter, and the modules with their associated converters are still connected in series to create a high dc voltage, which

is provided to a simplified dc/ac inverter. This approach combines aspects of string inverters and ac-module inverters and offers the advantages of individual module maximum power point (MPP) tracking (MPPT), but it is less costly and more efficient than ac-module inverters. However, there are two power conversion stages in this configuration. Another cascaded inverter is shown in Fig. 1(f), where each PV panel is connected to its own dc/ac inverter, and those inverters are then placed in series to reach a high-voltage level [13]–[16]. This cascaded inverter would maintain the benefits of “one converter per panel,” such as better utilization per PV module, capability of mixing different sources, and redundancy of the system. In addition, this dc/ac cascaded inverter removes the need for the per-string dc bus and the central dc/ac inverter, which further improves the overall efficiency.

The modular cascaded H-bridge multilevel inverter, which requires an isolated dc source for each H-bridge, is one dc/ac cascaded inverter topology. The separate dc links in the multilevel inverter make independent voltage control possible. As a result, individual MPPT control in each PV module can be achieved, and the energy harvested from PV panels can be maximized. Meanwhile, the modularity and low cost of

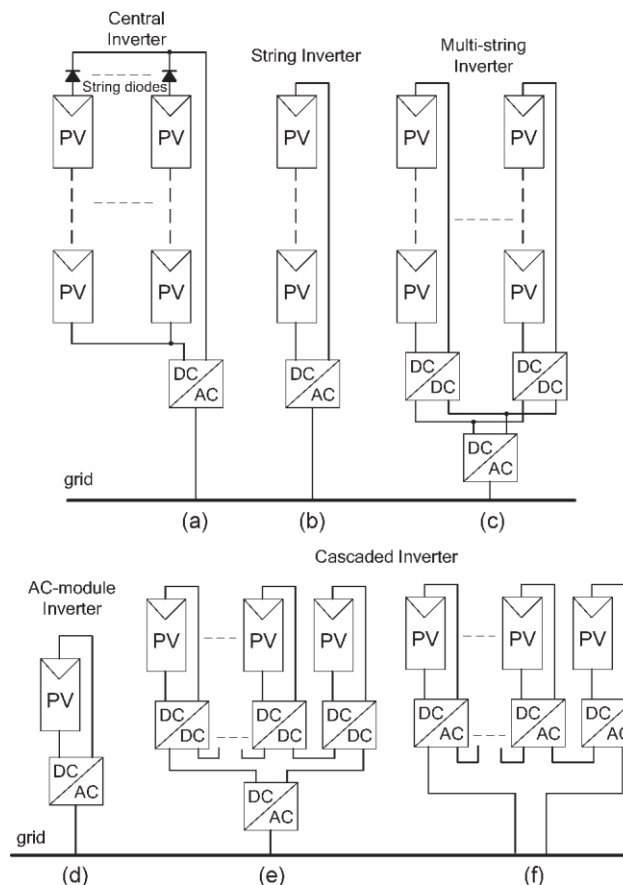


Fig. 1. Configurations of PV systems. (a) Central inverter. (b) String inverter. (c) Multistring inverter. (d) AC-module inverter. (e) Cascaded dc/dc converter. (f) Cascaded dc/ac inverter

multilevel converters would position them as a prime candidate. for the next generation of efficient, robust, and reliable grid- connected solar power electronics.

A modular cascaded H-bridge multilevel inverter topology for single- or three-phase grid-connected PV systems is pre- sented in this paper. The panel mismatch issues are addressed to show the necessity of individual MPPT control, and a control scheme with distributed MPPT control is then proposed. The distributed MPPT control scheme can be applied to both single- and three-phase systems.

In addition, for the presented three-phase grid-connected PV system, if each PV module is operated at its own MPP, PV mismatches may introduce unbalanced power supplied to the three-phase multilevel inverter, leading to unbalanced injected grid current. To balance the three-phase grid current, modula- tion compensation is also added to the control system.

A three-phase modular cascaded multilevel inverter proto- type has been built. Each H-bridge is connected to a 185-W solar panel. The modular design will increase the flexibility of the system and

reduce the cost as well. Simulation and experimental results are provided to demonstrate the developed control scheme

## II. SYSTEM DESCRIPTION

Modular cascaded H-bridge multilevel inverters for single- and three-phase grid-connected PV systems are shown in Fig. 2 Each phase consists of  $n$  H-bridge converters connected in series, and the dc link of each H-bridge can be fed by a PV panel or a short string of PV panels. The cascaded multilevel inverter is connected to the grid through  $L$  filters, which are used to reduce the switching harmonics in the current.

By different combinations of the four switches in each H-bridge module, three output voltage levels can be generated:

$-v_{dc}$ , 0, or  $+v_{dc}$ . A cascaded multilevel inverter with  $n$  input sources will provide  $2n + 1$  levels to synthesize the ac output waveform. This  $(2n + 1)$ -level voltage waveform enables the reduction of harmonics in the synthesized current, reducing the size of the needed output filters. Multilevel inverters also have other advantages such as reduced voltage stresses on the semiconductor switches and having higher efficiency when compared to other converter topologies [17].

## III. PANEL MISMATCHES

PV mismatch is an important issue in the PV system. Due to the unequal received irradiance, different temperatures, and aging of the PV panels, the MPP of each PV module may be different. If each PV module is not controlled independently, the efficiency of the overall PV system will be decreased.

To show the necessity of individual MPPT control, a five-level two-H-bridge single-phase inverter is simulated in MATLAB/SIMULINK. Each H-bridge has its own 185-W PV panel connected as an isolated dc source. The PV panel is modeled according to the specification of the commercial PV panel from Astronergy CHSM-5612M.

Consider an operating condition that each panel has a different irradiation from the sun; panel 1 has irradiance  $S = 1000 \text{ W/m}^2$ , and panel 2 has  $S = 600 \text{ W/m}^2$ . If only panel 1 is tracked and its MPPT controller determines the average voltage of the two panels, the power extracted from panel 1 would be 133 W, and the power from panel 2 would be 70 W, as can be seen in Fig. 3. Without individual MPPT control, the total power harvested from the PV system is 203 W.

However, Fig. 4 shows the MPPs of the PV panels under the different irradiance. The maximum output power values will be 185 and 108.5 W when the  $S$  values are 1000 and  $600 \text{ W/m}^2$ , respectively, which means that the total power harvested from the PV system would be 293.5 W if individual MPPT can be achieved. This higher value is about 1.45 times of the one before. Thus, individual MPPT control in each PV module is required to increase the efficiency of the PV system.

In a three-phase grid-connected PV system, a PV mismatch may cause more problems. Aside from decreasing the overall efficiency, this could even introduce unbalanced power supplied to the three-phase grid-connected system. If there are PV mismatches between phases, the input power of each phase would be different. Since the grid voltage is balanced, this difference in input power will cause unbalanced current to the grid, which is not allowed by grid standards. For example, to unbalance the current per phase more than 10% is not allowed for some utilities, where the percentage imbalance is calculated by taking the maximum deviation from the average current and dividing it by the average current [18].

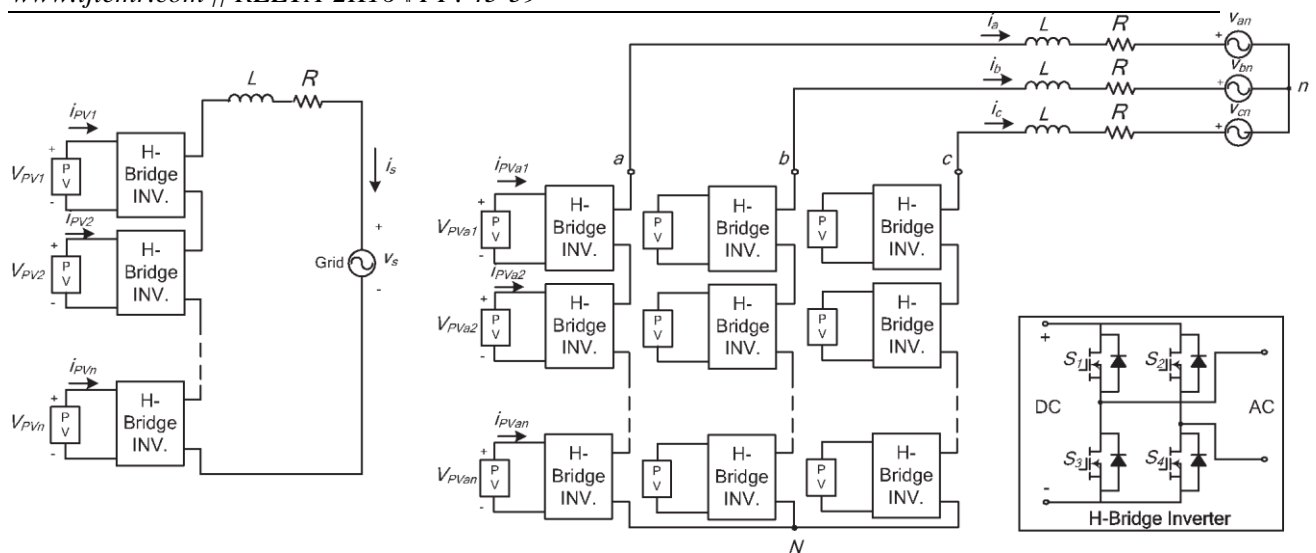


Fig. 2. Topology of the modular cascaded H-bridge multilevel inverter for grid-connected PV systems

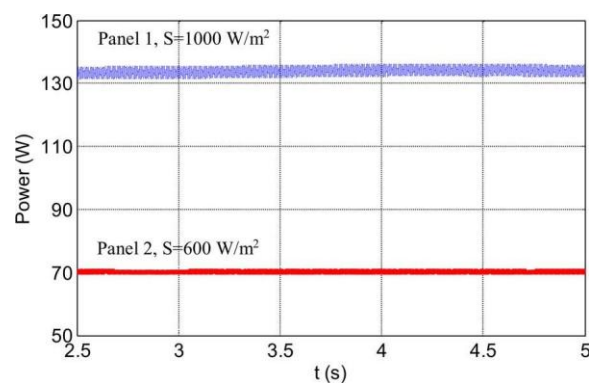


Fig. 3. Power extracted from two PV panels.

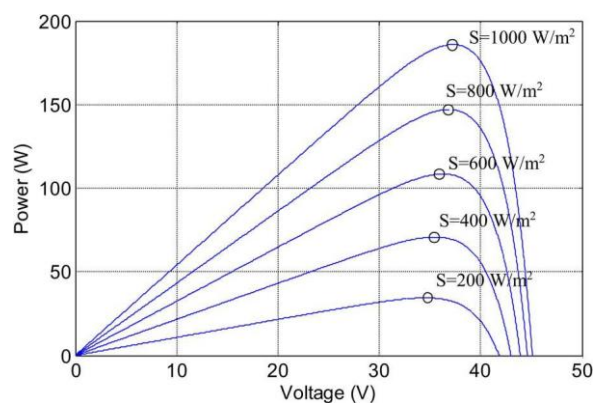


Fig. 4.  $P-V$  characteristic under the different irradiance.

To solve the PV mismatch issue, a control scheme with individual MPPT control and modulation compensation is proposed. The details of the control scheme will be discussed in the next section.

#### IV. CONTROL SCHEME

##### A. Distributed MPPT Control

In order to eliminate the adverse effect of the mismatches and increase the efficiency of the PV system, the PV modules need to operate at different voltages to improve the utilization per PV module.

The separate dc links in the cascaded H-bridge multilevel inverter make independent voltage control possible. To realize individual MPPT control in each PV module, the control scheme proposed in

The distributed MPPT control of the three-phase cascaded H-bridge inverter is shown in Fig. 5. In each H-bridge module, an MPPT controller is added to generate the dc-link voltage reference. Each dc-link voltage is compared to the corresponding voltage reference, and the sum of all errors is controlled through a total voltage controller that determines the current reference  $I_{\text{dref}}$ . The reactive current reference  $I_{\text{qref}}$  can be set to zero, or if reactive power compensation is required,  $I_{\text{qref}}$  can also be given by a reactive current calculator [20]. The synchronous reference frame phase-locked loop (PLL) has been used to find the phase angle of the grid voltage. As the classic control scheme in three-phase systems, the grid currents in  $abc$  coordinates are converted to  $dq$  coordinates and regulated through proportional-integral (PI) controllers to generate the modulation index in the  $dq$  coordinates, which is then converted back to three phases.

To make each PV module operate at its own MPP, take phase  $a$  as an example; the voltages  $vdca2$  to  $vdcan$  are controlled individually through  $n - 1$  loops. Each voltage controller gives the modulation index proportion of one H-bridge module in phase  $a$ . After multiplied by the modulation index of phase  $a$ ,  $n - 1$  modulation indices can be obtained. Also, the modulation index for the first H-bridge can be obtained by subtraction. The control schemes in phases  $b$  and  $c$  are almost the same. The only difference is that all dc-link voltages are regulated through PI controllers, and  $n$  modulation index proportions are obtained for each phase

The diagram illustrates the control and power flow of a cascaded H-bridge inverter system. At the top, a PV source feeds a Cascaded H-Bridge Multilevel Inverter with  $n$  stages. Each stage consists of an LC filter (inductor  $L$ , capacitor  $C$ ) and a resistor  $R$ . The output voltages are  $V_{an}, V_{bn}, V_{cn}$ . The system is controlled by an SRF-PLL (Synchronous Reference Frame Phase-Locked Loop) which provides a reference angle  $\theta$  to an  $abc/dq$  converter. The  $abc/dq$  converter takes the grid voltages  $e_{va}, e_{vb}, e_{vc}$  and the reference angle  $\theta$  to produce the dq components  $i_d$  and  $i_q$ . These components are then used by a  $dq/abc$  converter to produce the reference currents  $i_{dref}$  and  $i_{qref}$ . The  $i_{dref}$  is compared with the feedback  $i_d$  and the error is processed by a PI controller to produce the reference current  $i_{dref}$ . The  $i_{qref}$  is compared with the feedback  $i_q$  and the error is processed by a PI controller to produce the reference current  $i_{qref}$ . The reference currents are then used by a Modulation compensation block to produce the modulation signals  $d'_a, d'_b, d'_c$ . The modulation signals are then used by a PS-SPWM (Pulse Width Modulation) block to generate the switching signals for the inverter. The PS-SPWM block also takes the reference currents  $i_{dref}$  and  $i_{qref}$  as inputs. The output of the PS-SPWM block is the switching signals  $S_{a1}, S_{a2}, \dots, S_{an}$ .

A phase-shifted sinusoidal pulse width modulation switching scheme is then applied to control the switching devices of each H-bridge.

As mentioned earlier, a PV mismatch may cause more problems to a three-phase modular cascaded H-bridge multi-level PV inverter. With the individual MPPT control in each H-bridge module, the input solar power of each phase would be different, which introduces unbalanced current to the grid. To solve the issue, a zero sequence voltage can be imposed upon the phase legs in order to affect the current flowing into each phase. If the updated inverter output phase voltage is proportional to the unbalanced power, the current

will be balanced.

Thus, the modulation compensation block, as shown in Fig. 6, is added to the control system of three-phase modular cascaded multilevel PV inverters. The key is how to update the modulation index of each phase without increasing the

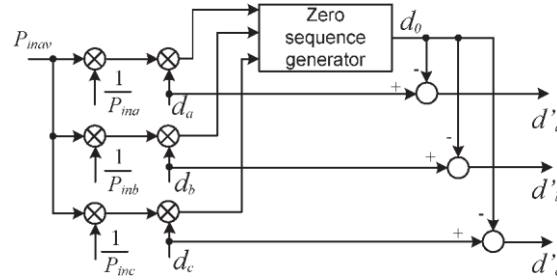


Fig. 6. Modulation compensation scheme.

complexity of the control system. First, the unbalanced power is weighted by ratio  $r_j$ , which is calculated as

$$r_j = \frac{P_{inav}}{P_{inj}} \quad (1)$$

where  $P_{inj}$  is the input power of phase  $j$  ( $j = a, b, c$ ), and  $P_{inav}$  is the average input power.

Then, the injected zero sequence modulation index can be generated as

$$d_0 = \frac{1}{2} [\min(r_a d_a, r_b d_b, r_c d_c) + \max(r_a d_a, r_b d_b, r_c d_c)] \quad (2)$$

where  $d_j$  is the modulation index of phase  $j$  ( $j = a, b, c$ ) and is determined by the current loop controller.

The modulation index of each phase is updated by

$$d'_j = d_j - d_0. \quad (3)$$

Only simple calculations are needed in the scheme, which will not increase the complexity of the control system. An example is presented to show the modulation compensation scheme more clearly. Assume that the input power of each phase is unequal

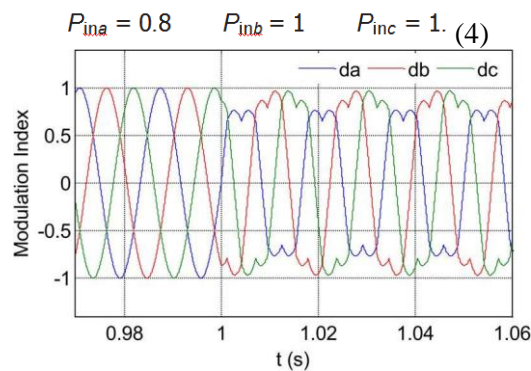


Fig. 7. Modulation indices before and after modulation compensation.



TABLE I SYSTEM PARAMETERS

Parameters	Value
DC-link capacitor	3600 $\mu$ F
Connection inductor $L$	2.5 mH
Grid resistor $R$	0.1 ohm
Grid rated phase voltage	60 Vrms
Switching frequency	1.5 kHz

By injecting a zero sequence modulation index at  $t = 1$  s, the balanced modulation index will be updated, as shown in Fig. 7. It can be seen that, with the compensation, the updated modulation index is unbalanced proportional to the power, which means that the output voltage ( $v_{jN}$ ) of the three-phase inverter is unbalanced, but this produces the desired balanced grid current.

## V. SIMULATION RESULT

Simulation and experimental tests are carried out to validate the proposed ideas. A modular cascaded multilevel inverter prototype has been built in the laboratory. The MOSFET IRFSL4127 is selected as inverter switches operating at 1.5 kHz. The control signals to the H-bridge inverters are sent by a dSPACE ds1103 controller.

A three-phase seven-level cascaded H-bridge inverter is simulated and tested. Each H-bridge has its own 185-W PV panel (Astronergy CHSM-5612M) connected as an independent source. The inverter is connected to the grid through a transformer, and the phase voltage of the secondary side is 60 Vrms. The system parameters are shown in Table I.

### A. Simulation Results

To verify the proposed control scheme, the three-phase grid-connected PV inverter is simulated in two different conditions. First, all PV panels are operated under the same irradiance  $S = 1000$  W/m<sup>2</sup> and temperature  $T = 25$  °C. At  $t = 0.8$  s, the solar irradiance on the first and second panels of phase  $a$  decreases to 600 W/m<sup>2</sup>, and that for the other panels stays the same. The dc-link voltages of phase  $a$  are shown in Fig. 8. At the beginning, all PV panels are operated at an MPP voltage of 36.4 V. As the irradiance changes, the first and second dc-link voltages decrease and track the new MPP voltage of 36 V, while the third panel is still operated at 36.4 V.

The PV current waveforms of phase  $a$  are shown in Fig. 9. After  $t = 0.8$  s, the currents of the first and second PV panels are much smaller due to the low irradiance, and the lower ripple of the dc-link voltage can be found in Fig. 8(a).

The dc-link voltages of phase  $b$  are shown in Fig. 10. All phase- $b$  panels track the MPP voltage of 36.4 V, which shows that they are not influenced by other phases. With the distributed MPPT control, the dc-link voltage of each H-bridge can be controlled independently. In other words, the connected PV panel of each H-bridge can be operated at its own MPP voltage and will not be influenced by the panels connected to other H-bridges. Thus, more solar energy can be extracted, and the efficiency of the overall PV system will be increased.

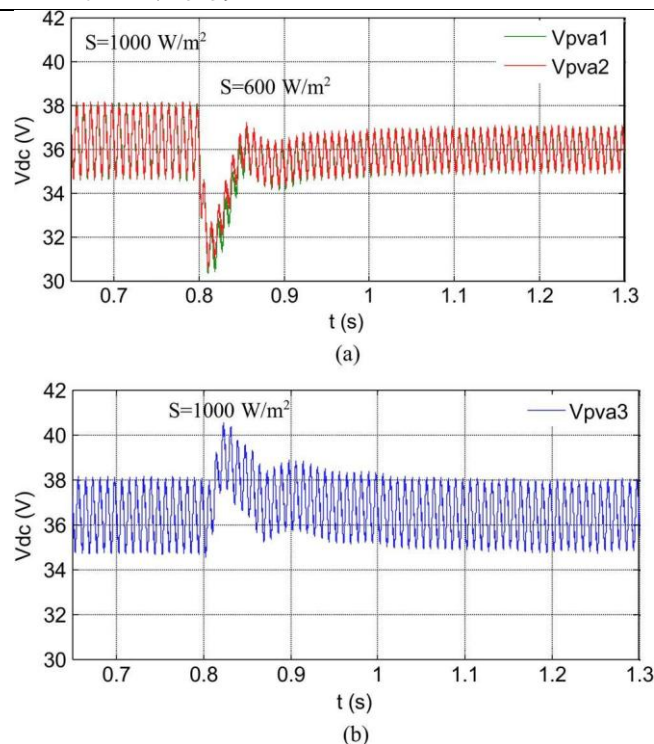


Fig. 8. DC-link voltages of phase *a* with distributed MPPT ( $T = 25^\circ\text{C}$ ).  
 (a) DC-link voltage of modules 1 and 2. (b) DC-link voltage of module 3.

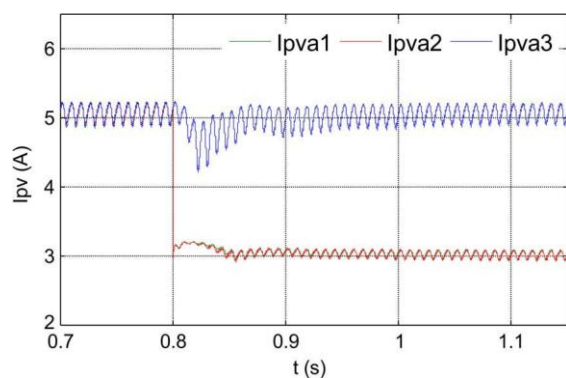


Fig. 9. PV currents of phase *a* with distributed MPPT ( $T = 25^\circ\text{C}$ ).

Fig. 11 shows the power extracted from each phase. At the beginning, all panels are operated under irradiance

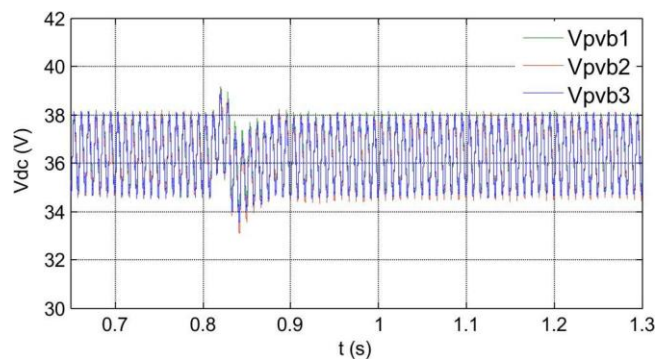


Fig. 10. DC-link voltages of phase *b* with distributed MPPT ( $T = 25^\circ\text{C}$ ).



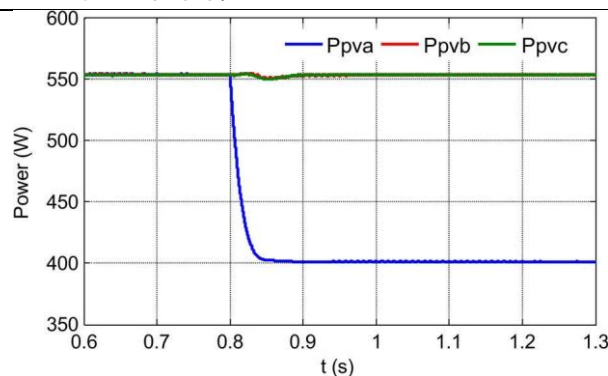


Fig. 11. Power extracted from PV panels with distributed MPPT.

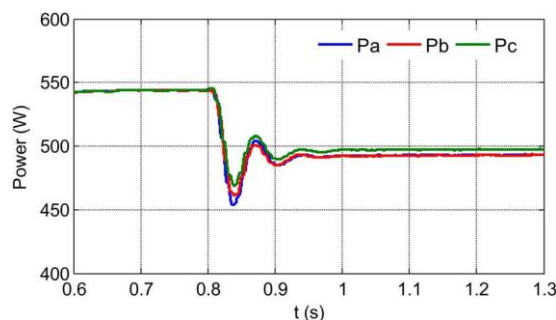


Fig. 12. Power injected to the grid with modulation compensation.

$S = 1000 \text{ W/m}^2$ , and every phase is generating a maximum power of 555 W. After  $t = 0.8 \text{ s}$ , the power harvested from phase  $a$  decreases to 400 W, and those from the other two phases stay the same. Obviously, the power supplied to the three-phase grid-connected inverter is unbalanced. However, by applying the modulation compensation scheme, the power injected to the grid is still balanced, as shown in Fig. 12. In addition, by comparing the total power extracted from the PV panels with the total power injected to the grid, it can be seen that there is no extra power loss caused by the modulation compensation scheme.

Fig. 13 shows the output voltages ( $v_{iN}$ ) of the three-phase inverter. Due to the injected zero sequence component, they are unbalanced after  $t = 0.8 \text{ s}$ , which help to balance the grid current shown in Fig. 14.

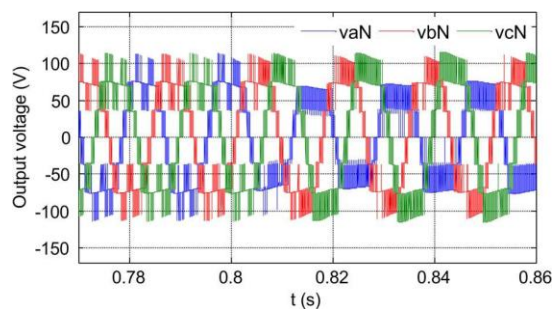


Fig. 13. Three-phase inverter output voltage waveforms with modulation compensation.

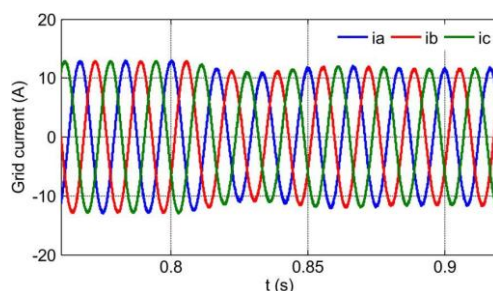


Fig. 14. Three-phase grid current waveforms with modulation compensation.

## B. Simulation Verification

A three-phase seven-level cascaded H-bridge inverter has been built by nine H-bridge modules (three modules per phase) in the laboratory. Fig. 15 shows the experimental solar panels and the three-phase modular cascaded multilevel inverter. As mentioned previously, the dc link of each H-bridge module is fed by one PV panel Astronergy CHSM-5612M.

To validate the proposed control scheme, the three-phase grid-connected PV inverter has been tested under different conditions. In the tests, cards with different sizes are placed on top of PV panels to provide partial shading, which effectively changes the solar irradiance.

*Test 1:* A small blue card (9 cm × 7 cm) is placed on the third panel of phase *a*, and one cell of the panel is partly covered, as shown in Fig. 16.

The experimental results are presented in Figs. 17–21. Fig. 17 shows three dc-link voltages of phase *a*. The output voltage of each PV panel is controlled individually to track its own MPP voltage. Since the third panel is partly covered, its MPP voltage is a little lower. The PV current waveforms of phase *a* are shown in Fig. 18. The PV current of the third panel is smaller due to the card covering. However, the first and second panels are operated at their own MPPs, and their PV currents are not influenced. With the individual MPPT control, the efficiency loss caused by PV mismatches can be prevented. As shown in Fig. 17, there is a second-order harmonic in the output voltage of the PV panels. So, the second-order harmonic is also seen in the output current of the PV panels. In addition, to have a high utilization ratio of 99% of PV modules, the voltage ripple should be less than 6% of the MPP voltage. In this

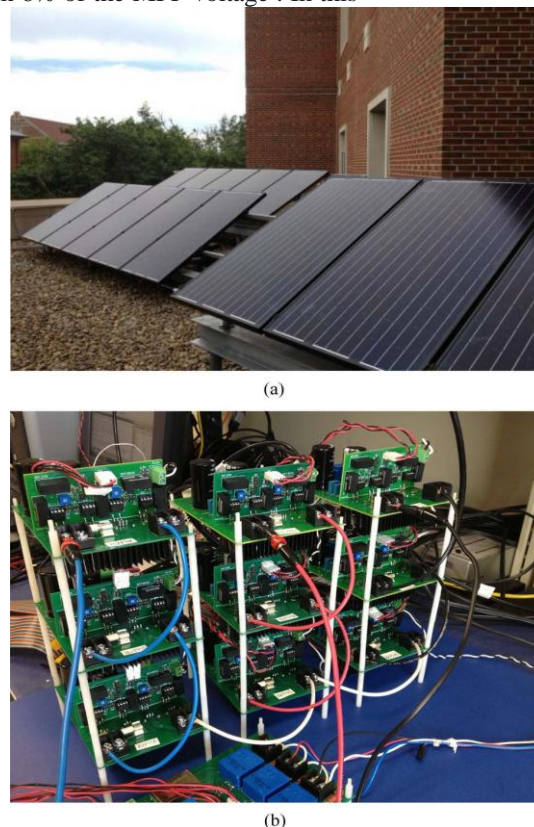


Fig. 15. Experimental prototype. (a) Solar panels Astronergy CHSM-5612M.  
(b) Modular three-phase seven-level cascaded H-bridge inverter.



Fig. 16. PV panels of phase *a*: One cell of the third panel is partly covered.

test, the voltage ripple is about 1.8 V, which is less than 6% of the MPP voltage.

Fig. 19 shows the solar power extracted from each phase, which is unbalanced. To balance the injected grid current, the

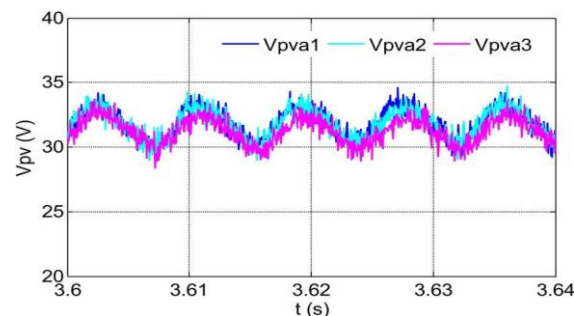


Fig. 17. DC-link voltages of phase *a*.

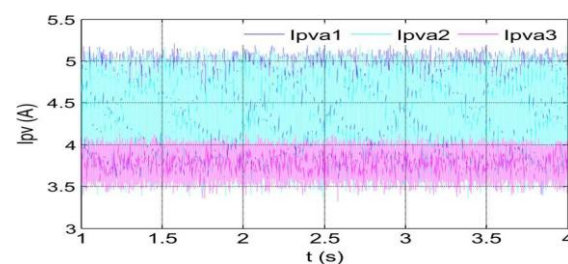


Fig. 18. PV currents of phase *a* (test 1).

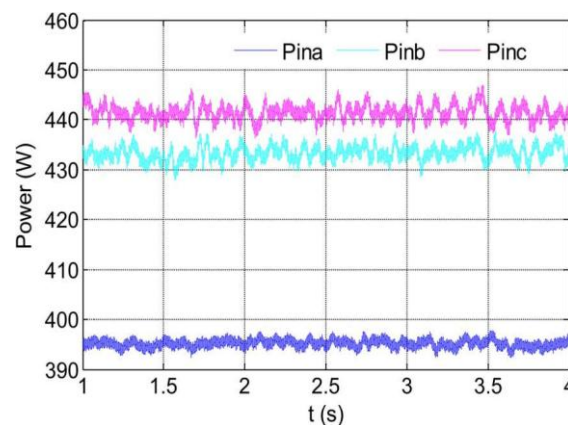


Fig. 19. Experimental power extracted from PV panels with distributed MPPT (test 1).

modulation compensation scheme proposed here is applied. As presented in Fig. 20, a zero sequence voltage is imposed upon the phase legs. The inverter output voltage ( $v_{jN}$ ) is unbalanced proportional to the supplied power of each phase, which helps to balance the grid current. Fig. 21 shows the three-phase grid current waveforms. Even if PV mismatch happens and the supplied PV power to the three-phase system is unbalanced, the three-phase grid current is still balanced.

The THD of the grid current shown in Fig. 21 is 3.3%, as shown in Fig. 22.

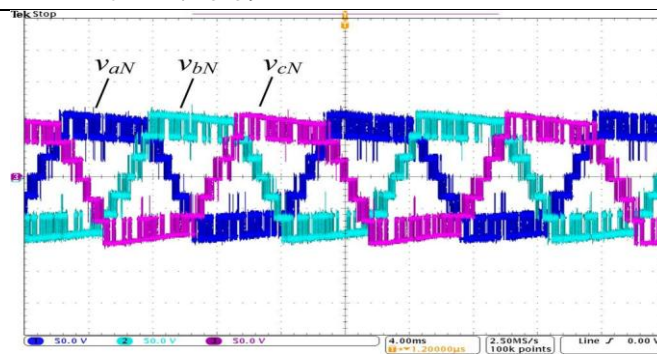


Fig. 20. Experimental inverter output voltages with modulation compensation (test 1).

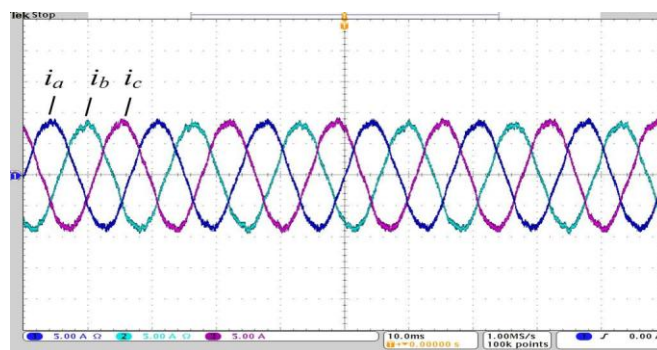


Fig. 21. Experimental grid currents with unbalanced PV power (test 1).

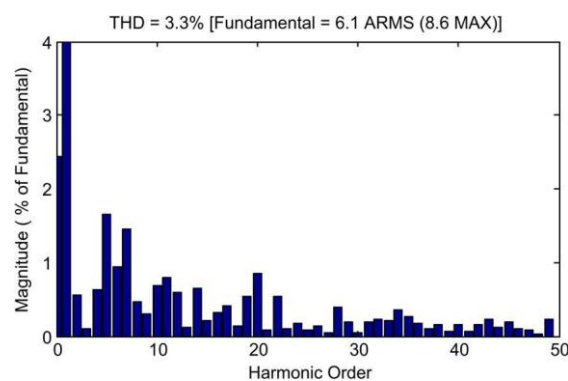


Fig. 22. THD of the grid current shown in Fig. 21 (test 1).

*Test 2:* A large blue card (13.5 cm × 9 cm) is placed on the third panel of phase *a*, and one cell of the panel is almost fully covered, as shown in Fig. 23.

Fig. 24 shows the PV current waveforms of phase *a*. Since one cell of the third panel is almost fully covered, the current of the panel drops to 2 A, while the currents of the other two panels in the same phase are still 4 A.

The harvested solar power of each phase is shown in Fig. 25. Compared to test 1, the power supplied to the three-phase sys-



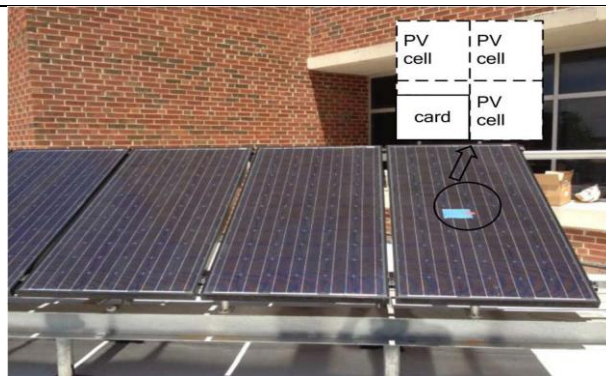


Fig. 23. PV panels of phase  $a$ : One cell of the third panel is covered.

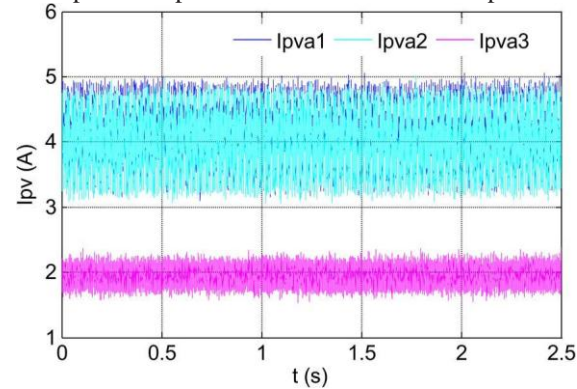


Fig. 24. Experimental PV currents of phase  $a$  (test 2).

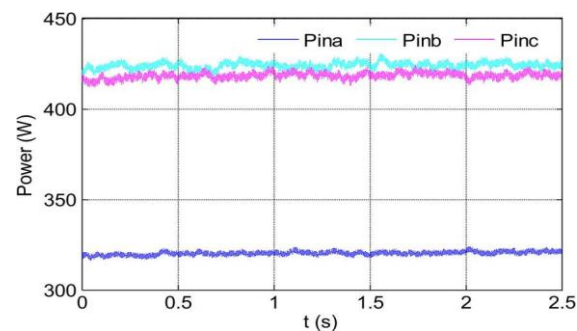


Fig. 25. Experimental power extracted from PV panels with distributed MPPT (test 2).

tem is more unbalanced. However, the three-phase grid current can still be balanced by applying the modulation compensation, as presented in Fig. 26. The THD of the grid current is 4.2%, and the rms value is 5.5 A.

Fig. 27 shows the inverter output voltage waveforms. As discussed earlier, the inverter output voltage ( $v_{jN}$ ) is unbalanced proportional to the supplied solar power of each phase to help balance the grid current. Thus, the output voltages  $v_{bN}$  (76.0 Vrms) and  $v_{cN}$  (75.2 Vrms) are higher than  $v_{aN}$  (57.9 Vrms).

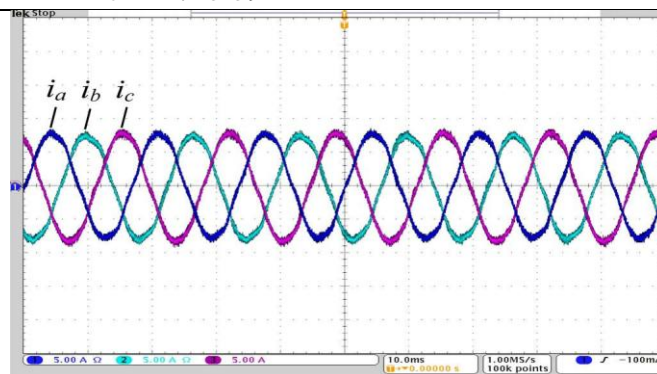


Fig. 26. Experimental grid currents with unbalanced PV power (test 2).

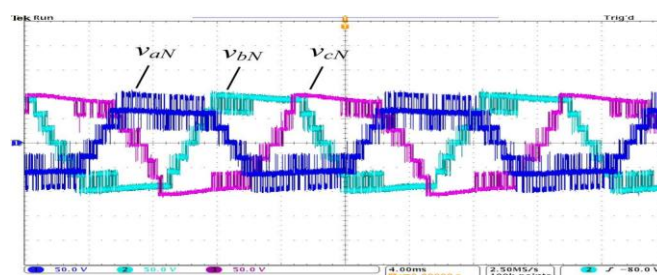


Fig. 27. Experimental inverter output voltages with modulation compensation (test 2).

#### IV. CONCLUSION

In this paper, a modular cascaded H-bridge multilevel in-verter for grid-connected PV applications has been presented. The multilevel inverter topology will help to improve the utilization of connected PV modules if the voltages of the separate dc links are controlled independently. Thus, a distributed MPPT control scheme for both single- and three-phase PV systems has been applied to increase the overall efficiency of PV systems. For the three-phase grid-connected PV system, PV mismatches may introduce unbalanced supplied power, resulting in unbalanced injected grid current. A modulation compensation scheme, which will not increase the complexity of the control system or cause extra power loss, is added to balance the grid current.

A modular three-phase seven-level cascaded H-bridge in-verter has been built in the laboratory and tested with PV panels under different partial shading conditions. With the proposed control scheme, each PV module can be operated at its own MPP to maximize the solar energy extraction, and the three-phase grid current is balanced even with the unbalanced supplied solar power.

#### REFERENCES

- [1]. J. M. Carrasco *et al.*, "Power-electronic systems for the grid integration of renewable energy sources: A survey," *IEEE Trans. Ind. Electron.*, vol. 53, no. 4, pp. 1002–1016, Jun. 2006.
- [2]. S. B. Kjaer, J. K. Pedersen, and F. Blaabjerg, "A review of single-phase grid connected inverters for photovoltaic modules," *IEEE Trans. Ind. Appl.*, vol. 41, no. 5, pp. 1292–1306, Sep./Oct. 2005.
- [3]. M. Meinhardt and G. Cramer, "Past, present and future of grid connected photovoltaic- and hybrid power-systems," in *Proc. IEEE PES Summer Meet.*, 2000, vol. 2, pp. 1283–1288.
- [4]. M. Calais, J. Myrzik, T. Spooner, and V. G. Agelidis, "Inverter for single-phase grid connected photovoltaic systems—An overview," in *Proc. IEEE PESC*, 2002, vol. 2, pp. 1995–2000.
- [5]. J. M. A. Myrzik and M. Calais, "String and module integrated inverters for single-phase grid connected photovoltaic systems—A review," in *Proc. IEEE Bologna Power Tech Conf.*, 2003, vol. 2, pp. 1–8.
- [6]. F. Schimpf and L. Norum, "Grid connected converters for photovoltaic, state of the art, ideas for improvement of transformerless inverters," in *Proc. NORPIE*, Espoo, Finland, Jun. 2008, pp. 1–6.
- [7]. B. Liu, S. Duan, and T. Cai, "Photovoltaic DC-building-module-based BIPV system—Concept and design considerations," *IEEE Trans. Power Electron.*, vol. 26, no. 5, pp. 1418–1429, May 2011.
- [8]. L. M. Tolbert and F. Z. Peng, "Multilevel converters as a utility interface for renewable energy systems," in *Proc. IEEE Power Eng. Soc. Summer Meet.*, Seattle, WA, USA, Jul. 2000, pp. 1271–



- 1274.
- [9]. H. Ertl, J. Kolar, and F. Zach, "A novel multicell DC–AC converter for applications in renewable energy systems," *IEEE Trans. Ind. Electron.*, vol. 49, no. 5, pp. 1048–1057, Oct. 2002.
  - [10]. S. Daher, J. Schmid, and F. L. M. Antunes, "Multilevel inverter topologies for stand-alone PV systems," *IEEE Trans. Ind. Electron.*, vol. 55, no. 7, pp. 2703–2712, Jul. 2008.
  - [11]. G. R. Walker and P. C. Sernia, "Cascaded DC–DC converter connection of photovoltaic modules," *IEEE Trans. Power Electron.*, vol. 19, no. 4, pp. 1130–1139, Jul. 2004.
  - [12]. E. Roman, R. Alonso, P. Ibanez, S. Elorduizaparietxe, and D. Goitia, "Intelligent PV module for grid-connected PV systems," *IEEE Trans. Ind. Electron.*, vol. 53, no. 4, pp. 1066–1073, Jun. 2006.
  - [13]. F. Filho, Y. Cao, and L. M. Tolbert, "11-level cascaded H-bridge grid- tied inverter interface with solar panels," in *Proc. IEEE APEC Expo.*, Feb. 2010, pp. 968–972.
  - [14]. C. D. Townsend, T. J. Summers, and R. E. Betz, "Control and modulation scheme for a cascaded H-bridge multi-level converter in large scale photovoltaic systems," in *Proc. IEEE ECCE*, Sep. 2012, pp. 3707–3714.
  - [15]. B. Xiao, L. Hang, and L. M. Tolbert, "Control of three-phase cascaded voltage source inverter for grid-connected photovoltaic systems," in *Proc. IEEE APEC Expo.*, Mar. 2013, pp. 291–296.
  - [16]. Y. Zhou, L. Liu, and H. Li, "A high-performance photovoltaic module- integrated converter (MIC) based on cascaded quasi-Z-source inverters (qZSI) using eGaN FETs," *IEEE Trans. Power Electron.*, vol. 28, no. 6, pp. 2727–2738, Jun. 2013.
  - [17]. J. Rodriguez, J. S. Lai, and F. Z. Peng, "Multilevel inverters: A survey of topologies, controls, and applications," *IEEE Trans. Ind. Electron.*, vol. 49, no. 4, pp. 724–738, Aug. 2002.
  - [18]. Standard for Electric Installation and Use. [Online]. Available: [https:// www.xcelenergy.com/](https://www.xcelenergy.com/)
  - [19]. A. Dell'Aquila, M. Liserre, V. Monopoli, and P. Rotondo, "Overview of PI-based solutions for the control of DC buses of a single-phase H-bridge multilevel active rectifier," *IEEE Trans. Ind. Appl.*, vol. 44, no. 3, pp. 857– 866, May/Jun. 2008.
  - [20]. B. Xiao, K. Shen, J. Mei, F. Filho, and L. M. Tolbert, "Control of cascaded H-bridge multilevel inverter with individual MPPT for grid-connected photovoltaic generators," in *Proc. IEEE ECCE*, Sep. 2012, pp. 3715– 3